

# Motility-associated hair-bundle motion in mammalian outer hair cells

Shuping Jia & David Z Z He

Mammalian hearing owes its remarkable sensitivity and frequency selectivity to a local mechanical feedback process within the cochlea. Cochlear outer hair cells (OHCs) function as the key elements in the feedback loop in which the fast somatic motility of OHCs is thought to be the source of cochlear amplification. An alternative view is that amplification arises from active hair-bundle movement, similar to that seen in nonmammalian hair cells. We measured voltage-evoked hair-bundle motions in the gerbil cochlea to determine if such movements were also present in mammalian OHCs. The OHCs showed bundle movement with peak responses of up to 830 nm. The movement was insensitive to manipulations that would normally block mechanotransduction in the stereocilia, and it was absent in neonatal OHCs and prestin-knockout OHCs. These findings suggest that the bundle movement originated in somatic motility and that somatic motility has a central role in cochlear amplification in mammals.

It is generally believed that mechanical amplification by hair cells is necessary to enhance the sensitivity and frequency-selectivity of hearing. In the mammalian cochlea, OHCs function as the key elements in a mechanical feedback loop that most likely involves the OHCs, organ of Corti micromechanics and the tectorial membrane (TM), with inner hair cells (IHCs) responding to the output of the feedback loop<sup>1,2</sup>. OHCs have a voltage-dependent length change termed electromotility<sup>3,4</sup>. This somatic motility, when driven by the receptor potential *in vivo*, is thought to underlie cochlear amplification in mammals<sup>1–5</sup>. An alternative view is that the amplification arises from active hair-bundle motion<sup>6,7</sup>. Active hair-bundle movements ranging between 5 and 80 nm have been observed in several nonmammalian species and can occur spontaneously with amplitudes in excess of that expected for Brownian motion<sup>8–10</sup>. Such movements have also been observed as reactions to hair-bundle displacement with compliant probes<sup>8,11–13</sup>, and in response to changes in membrane potential<sup>18,9,13–15</sup>. The active hair-bundle movements, intimately related to the reclosure of the mechanotransducer channels<sup>8,13</sup> and the myosin motors<sup>11,16,17</sup> involved in adaptation, can produce forces that amplify mechanical stimuli<sup>6,7</sup>. The movements are sensitive to extracellular calcium concentration and can be altered by calcium influx through mechano-electrical transducer channels<sup>8,13,15–17</sup>.

Active hair-bundle motion has been shown to produce all of the characteristics of the active process in non-mammals, but two recent studies<sup>18,19</sup> indicate that hair-bundle motion may also have an important role in cochlear amplification in mammals. One study, using a two-chamber *in vitro* cochlear preparation of gerbils, showed that nonlinear amplification depends on calcium current through the mechano-electrical transducer channels<sup>18</sup>. Small hair-bundle motions of inner hair cells were observed in the same study. Another study

shows that hair bundles of rat OHCs can produce force on a submillisecond timescale<sup>19</sup>. The force, with a magnitude on the order of 500 pN, is linked to adaptation of the mechanotransducer channels<sup>19</sup>. To date, however, bundle motion has not been thoroughly examined in mammalian OHCs. To determine whether hair-bundle movements are also present in mammalian OHCs, we evaluated voltage-evoked hair-bundle activity in the cochlea of gerbils and prestin knockout mice<sup>5</sup>. We found that OHCs show bundle movement with peak responses of up to 830 nm. The movement was insensitive to manipulations that would normally block mechanotransduction in the stereocilia, and it was absent in neonatal OHCs and prestin-knockout OHCs. This result suggests that the bundle movement, under the conditions we studied, was not based on mechanotransducer channels but originated in somatic motility. The motility-associated response seems to overshadow transducer channel-based mechanisms in OHCs.

## RESULTS

Sensory epithelia were dissected from the cochleae of adult gerbils and prestin-knockout mice. The resulting coil preparation was bathed in artificial perilymph and viewed under a water-immersion objective microscope. The sensory epithelium was oriented with the hair bundles pointing up toward the objective. At high magnification, the hair bundles behaved as light pipes<sup>13</sup> and appeared as bright V-shaped lines under bright-field illumination (Fig. 1a). To measure bundle motion, the magnified (1,260×) image of the edge of the hair bundle was projected onto a photodiode through a rectangular slit. The photodiode-based system, mounted on the photo-port of the microscope, had a 3-dB cutoff frequency of 1,200 Hz and was capable of measuring motion down to roughly 5 nm with moderate averaging and low-pass filtering. Cells were selected if no obvious signs of deterioration in the

Hair Cell Biophysics Laboratory, Department of Biomedical Sciences, Creighton University School of Medicine, 2500 California Plaza, Omaha, Nebraska 68175, USA. Correspondence should be addressed to D.Z.Z.H. (hed@creighton.edu).

Published online 24 July 2005; doi:10.1038/nn1509

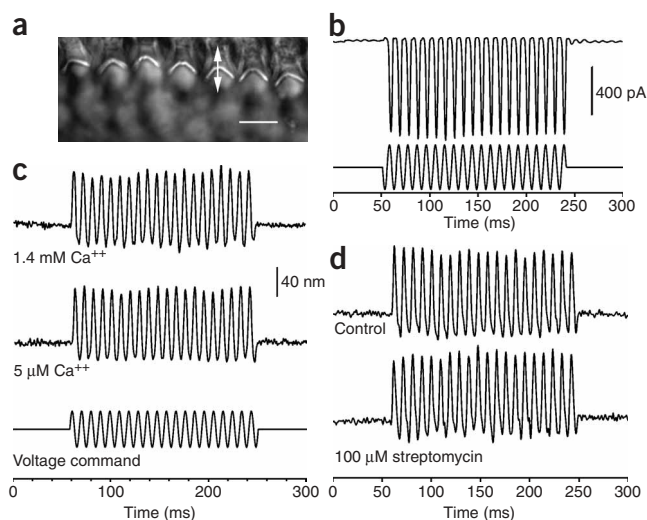


**Figure 1** Mechanotransducer current and hair-bundle motion of gerbil OHCs. (a) Hair bundles of OHCs under high magnification ( $63\times$  water-immersion objective) with bright field illumination. The bundles behaved as light pipes and appeared as bright V-shaped lines when focused at their tips. Double-headed arrow indicates the direction of bundle motion. Scale bar,  $10\ \mu\text{m}$ . (b) Mechanotransducer currents recorded from a gerbil apical-turn OHC from the coil preparation. The bundle was deflected by an oscillating stream from a fluid jet (tip diameter  $\sim 10\ \mu\text{m}$ ) positioned roughly  $20\text{--}30\ \mu\text{m}$  away from the bundle. The response shown is the average of three trials. The voltage command (102 Hz) to drive the water jet is presented at the bottom of the panel. Inward current is plotted downward. (c) Voltage-evoked bundle motions of a gerbil OHC at two different extracellular calcium concentrations. The 102-Hz voltage command varied the membrane potential from  $-100$  to  $-40$  mV around a holding potential of  $-70$  mV. Positive bundle motion (toward tall cilia) is plotted upward in this and all subsequent figures. (d) Bundle motion before and after perfusion of  $100\ \mu\text{M}$  streptomycin into the OHC stereociliary region. The responses in c and d were the averages of 100 trials. The scale bar in c also applies to the responses in d.

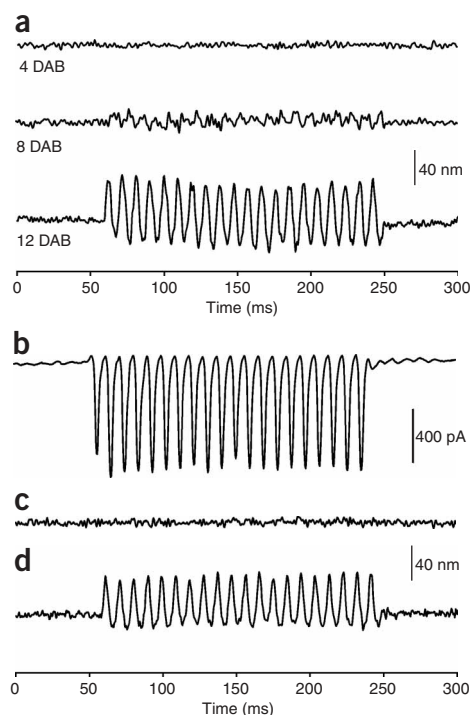
soma and/or hair bundle were visible at high magnification. Before the voltage-evoked bundle motion was measured, we recorded mechanotransducer currents to verify that the mechanotransducer apparatus in the stereocilia was not damaged. **Figure 1b** shows an example of such recording from a gerbil apical-turn OHC. The hair bundle was deflected by a fluid jet (with pipette tip diameter of  $10\ \mu\text{m}$ ) positioned  $20\text{--}30\ \mu\text{m}$  away from the bundle. Large transducer currents were recorded at the holding potential of  $-70$  mV in the voltage-clamp mode (**Fig. 1b**). The size of the current was comparable to that observed in previous studies in mammalian OHCs<sup>20–22</sup>. To determine bundle motions, we applied sinusoidal voltage bursts (102 Hz) to the OHCs through the patch electrode. The voltage command varied the membrane potential from  $-100$  mV to  $-40$  mV, from a holding potential of  $-70$  mV. Examples of the voltage-evoked hair-bundle movements are shown in **Fig. 1c** (see **Supplementary Videos 1,2** for large bundle motion). The observed bundle motion was asymmetrical, with larger bundle motions evoked by depolarization in the direction toward the tallest stereocilia (defined as positive bundle motion) than that evoked by hyperpolarization in the opposite direction (negative bundle motion). The direction of bundle motion during membrane potential change was consistent with that seen in turtle hair cells<sup>8,13</sup>, but it was of opposite polarity to that seen in bullfrog saccular hair cells<sup>14,15</sup>.

Hair cells of several nonmammalian species show active hair-bundle motion in response to changes in membrane potential<sup>8,9,13–15</sup>. The active motion, intimately associated with mechanotransducer channel apparatus, is secondary to alteration of calcium influx in the stereocilia and is therefore dependent on the extracellular calcium concentration<sup>8,13</sup>. We sought to determine whether the bundle motion observed in OHCs operates on a similar basis. We examined bundle motion

when the extracellular calcium concentration was reduced to  $5\ \mu\text{M}$  (**Fig. 1c**). Voltage-evoked bundle motion was compared before and after the ciliary bundle of five cells was perfused with low-calcium medium. We found robust voltage-evoked bundle motion both before and after perfusion, with no statistically significant difference in magnitude. Streptomycin is known to block mechanotransducer channels<sup>20</sup> and eliminate active and spontaneous bundle motion<sup>13,15</sup>. We perfused the ciliary area with  $100\ \mu\text{M}$  streptomycin to determine whether it blocked the voltage-evoked bundle motion in OHCs. The bundle motion was not affected by streptomycin (**Fig. 1d**). Collectively, these results suggest that the observed OHC bundle motion is different from the voltage-evoked bundle motion seen in nonmammalian hair cells.

As an alternative to motility derived from mechanotransducer processes, it is possible that bundle motion arises as a consequence of

**Figure 2** Hair-bundle motion of neonatal gerbil OHCs and mouse OHCs. (a) Voltage-evoked bundle motions measured from 4-, 8- and 12-d-old gerbil OHCs. The voltage command is the same as shown in **Fig. 1c**. (b) Mechanotransducer currents recorded from an apical-turn OHC of a prestin-knockout mouse. The hair bundle was deflected by a fluid jet (with a tip diameter of  $10\ \mu\text{m}$ ) positioned roughly  $20\text{--}30\ \mu\text{m}$  away from the bundle. The cell was held at  $-70$  mV under the voltage-clamp condition. (c) Lack of voltage-evoked bundle motion from the prestin-knockout mouse OHC. (d) Voltage-evoked bundle motion of an apical-turn OHC from wild-type mouse. The stimulus waveform and voltage command for c and d are the same as those shown in **Fig. 1c**.



somatic motility. To examine this possibility, we studied voltage-evoked bundle motion in neonatal gerbil OHCs. Previous studies have shown that the onset of OHC motility occurs around 6–8 days after birth (DAB)<sup>23</sup>, whereas mechanotransducer apparatus and mechanotransducer current with fast and slow adaptation are apparent before birth in mouse hair cells<sup>24</sup>. Consequently, mechanotransduction in the hair bundle is mature well before the onset of OHC motility<sup>20,21</sup>. Voltage-evoked bundle motions of apical-turn OHCs were measured from developing gerbils at 4, 8 and 12 DAB (**Fig. 2a**). When mechanotransduction had developed and somatic motility had not yet developed at 4 DAB, no voltage-evoked bundle motion was detected ( $n = 10$ ), even though large transducer currents could be measured (data not shown). At 8 DAB, we observed small bundle motion in one of the eight cells examined. At 12 DAB, when all OHCs typically exhibit electromotility<sup>23</sup>, voltage-evoked bundle motion was detected in all seven cells studied, with a magnitude of approximately 72% of that of the adult OHCs with the same voltage stimulation. The facts that neonatal OHCs do not have voltage-evoked hair-bundle motion before the onset of motility and that the development of bundle movements correlates with the development of somatic motility suggest that bundle motion, in response to membrane potential change, is related to somatic motility.

OHC somatic motility is mediated by the voltage-sensitive, membrane-bound motor protein, prestin<sup>25</sup>. To directly test whether the observed large bundle motion was related to somatic motility of OHCs, we examined the voltage-evoked bundle motion in prestin-knockout mice<sup>5</sup>. Such experiments are also important to determine whether there is any small transducer channel-based bundle motion that is overshadowed by the dominant motility-associated bundle motion. These knockout mice have normal morphology of the hair bundles and normal mechanotransducer functions, with no OHC somatic motility<sup>5,26</sup>. We measured transducer currents first to confirm that their mechanotransducer channels were functional and not damaged. When we recorded the transducer current from an apical-turn OHC of the prestin knockout mouse, a large asymmetrical transducer current was observed (**Fig. 2b**). We measured the voltage-evoked bundle motion from those OHCs. No voltage-evoked bundle motion was seen in any of the 11 cells examined (**Fig. 2c**). In contrast, when the voltage-evoked bundle motion was measured from OHCs of wild-type mice, large bundle motions were seen in all cells studied (**Fig. 2d**). To rule out the possibility that the lack of bundle motion in the prestin-null OHCs was due to perilymph solution bathing the stereocilia, we measured the voltage-evoked bundle motion after perfusing the ciliary area with artificial endolymph in five additional prestin-null OHCs. This mimics the *in vivo* chemical condition. No voltage-evoked bundle motions were observed in any of the five cells examined. This confirms that the voltage-evoked bundle motion is indeed associated with somatic motility.

In coil preparations, or under *in vivo* conditions, OHCs are constrained by adjacent OHCs and by supporting cells. The physical

connection among neighboring OHCs provides a basis for mechanical interaction among OHCs. Indeed, the influence of somatic motility of a stimulated OHC on the adjacent OHC through mechanical coupling has been shown previously<sup>27,28</sup>. If the observed voltage-evoked hair-bundle motion is associated with somatic motility and the consequent rotation of the reticular lamina, then the bundle motion should also be detected from adjacent OHCs, despite the fact that they are not under direct electrical stimulation. We measured the bundle motion of the stimulated cell (Cell 1 in **Fig. 3a**) and the adjacent unstimulated cell (Cell 2) in the same row. The stimulated cell was held at  $-70$  mV, and its membrane potential varied from  $-145$  mV to  $5$  mV at  $102$  Hz. A large response with peak-to-peak magnitude of  $253$  nm was detected from the stimulated cell (**Fig. 3b**). Bundle motion was also observed from the adjacent unstimulated OHC (Cell 2), even though only Cell 1 was stimulated electrically. The magnitude of bundle motion of the adjacent cell was roughly one-half that of the stimulated OHC (**Fig. 3b**). OHC motility and axial stiffness are sensitive to turgor pressure<sup>3,29</sup>. When OHCs are mechanically constrained by neighboring OHCs and supporting cells, as is the case *in vivo* and in the coil preparation, the turgor pressure becomes even more important, due to the mechanical load, for the expression of OHC motility and for the motility-driven reticular lamina rotation. We manipulated the turgor pressure of the stimulated cell to determine whether the bundle motion was also sensitive to turgor pressure. We reduced the turgor pressure by applying negative pressure through the patch electrode. The bundle motion of the stimulated OHC disappeared (**Fig. 3c**). The bundle motion of the adjacent OHC also disappeared after the stimulated cell lost its turgor pressure. The existence of bundle motion of the adjacent OHC and disappearance of bundle motion after turgor pressure loss indicate that the bundle motion results from rotation of the reticular lamina, as a consequence of somatic motility.

Subsequently, we examined bundle motion as a function of membrane potential (input-output function). **Figure 4a** shows an example of the response measured from a gerbil apical-turn OHC when the membrane potential was stepped up and down from a holding potential of  $-70$  mV. The responses were asymmetrical and nonlinear,

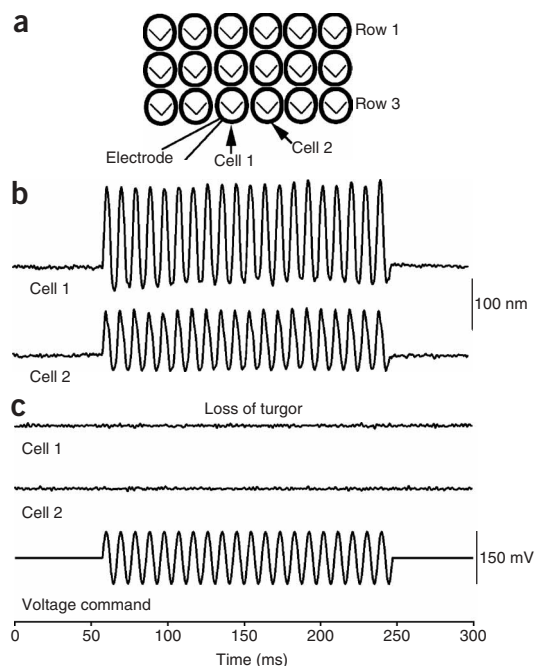


**Figure 3** Hair-bundle motion measured from a stimulated OHC and an adjacent unstimulated OHC. **(a)** Schematic drawing of method for recording bundle motions from a cell under voltage-clamp (Cell 1) and from an adjacent cell (Cell 2) that is not electrically stimulated but is mechanically coupled to Cell 1. **(b)** Bundle motion measured from Cell 1 and an adjacent cell (Cell 2). Cell 1 was held at  $-70$  mV and its membrane voltage varied from  $-145$  mV to  $5$  mV. Waveform is shown in the bottom panel of **c**. Note that large bundle motion was also observed from Cell 2, even though Cell 2 was not electrically stimulated. **(c)** Disappearance of voltage-evoked bundle motions in Cell 1 and Cell 2 after Cell 1 lost turgor pressure. Turgor pressure in Cell 1 was reduced by applying a negative pressure inside the patch electrode.

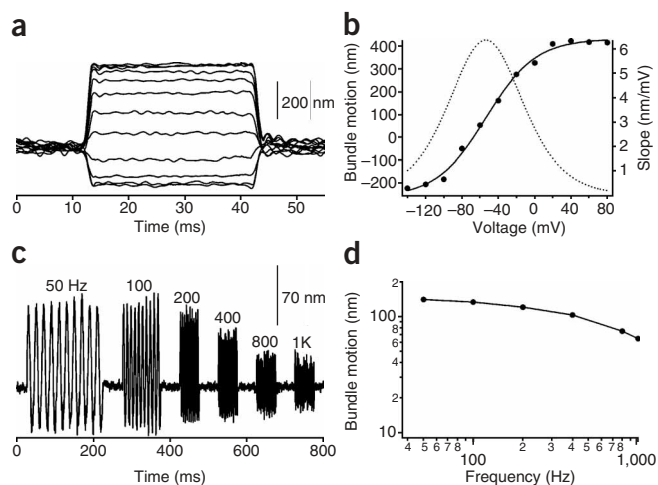


**Figure 4** Input-output function and frequency response of hair-bundle motion. **(a)** Bundle motions of a gerbil apical-turn OHC as a function of voltage level (from a holding potential of  $-70$  mV). **(b)** Steady-state response from **a** was fitted with a second-order Boltzmann function (solid line), and a slope function (dashed line) was obtained as the derivative of the Boltzmann function. The series resistance was 75% compensated. Because membrane conductances were blocked, the uncompensated voltage error (not corrected in the plot) was less than 4 mV at the largest voltage levels. The bundle motion was low-pass filtered at 400 Hz. **(c)** Motility-associated bundle motions evoked by a series of voltage bursts with different frequencies (frequency is shown on the top of the response waveforms). **(d)** The peak-to-peak response was measured from **c** and plotted as a function of frequency. The roll-off of the photodiode system was compensated in the frequency response. The response from the photodiode was low-pass filtered at 1,200 Hz.

with saturation in both directions, similar to that seen in OHC somatic motility<sup>29</sup>. We fitted the response with a second-order Boltzmann function; the maximum sensitivity calculated from the derivative of this function was about 6.2 nm/mV (**Fig. 3a**). The maximum peak-to-peak response shown in the example was 623 nm. The largest peak-to-peak response observed among the six cells examined was 832 nm (**Supplementary Videos 1,2**). We also examined the frequency response of the voltage-evoked bundle motion between 50 and 1,000 Hz using sinusoidal voltage bursts (**Fig. 4c**). Apparently, large bundle motions were still present at 1,000 Hz. The frequency response of the bundle motion was similar to that of OHC somatic motility measured under the whole-cell voltage-clamp condition<sup>30</sup>.

Finally, we attempted to quantify the relation between the bundle motion and somatic motility of OHCs. Since the bundle motion was measured in the coil preparation, where OHCs were loaded by neighboring OHCs and supporting cells, it was necessary to measure the change in OHC length under similar conditions. We measured the change in OHC length using a gerbil hemicochlear preparation<sup>31</sup>, which allowed us to measure motions of the cuticular plate and the hair bundle as a result of somatic motility from the same cells. The motion of the reticular lamina was measured in a previous study using an isolated cochlear preparation of the guinea pig<sup>32</sup>. Since the magnitude of reticular lamina motion depends on where the patch electrode holds the cells<sup>27</sup>, we chose to approach the basolateral

membrane of OHCs right above the nucleus to maximize the motion of the cuticular plate. Such measured motion should represent the total length change of OHCs *in situ* under the constrained condition. The response was asymmetrical and nonlinear, with saturation in both directions (**Fig. 5a**), similar to that seen in isolated OHCs<sup>29</sup>. The peak-to-peak magnitude of length change was about 1,384 nm, with a maximal sensitivity of 13 nm/mV (**Fig. 5b**). This value is similar to the maximal sensitivity of somatic motility (5–25 nm/mV) measured from isolated OHCs<sup>29</sup>. We also measured the bundle motion from the same cell with the same voltage stimulation. The bundle response measured from the hemicochlea resembled that measured from OHCs in the coil preparation (**Fig. 4a**). For comparison with OHC somatic motility, we plotted the steady-state response of the bundle motion as a function of voltage (**Fig. 5b**), along with its Boltzmann fit and the slope function. The slope sensitivity of bundle motion was about one-half of that of somatic motility. To quantify the relation between somatic motility and bundle motion, we plotted the magnitude of bundle motion as a function of somatic motility (**Fig. 5c**): the amplitude of bundle displacement was about one-half of the length change.

## DISCUSSION

Active hair-bundle motions are likely responsible for mechanical amplification of low-amplitude signals in non-mammals, since hair cells in these species do not possess somatic motility<sup>33</sup>. There is already evidence for either somatic motility or hair-bundle mechanisms in mammals. According to one recent study using a semi-intact cochlear preparation of adult gerbils, nonlinear amplification depends on the

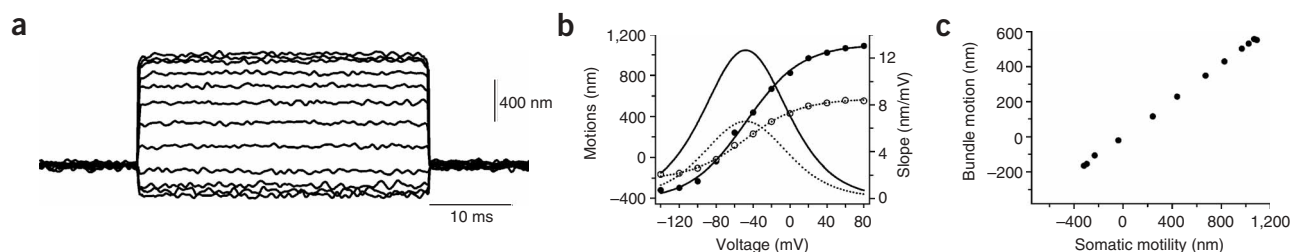


**Figure 5** Relationship between OHC somatic motility and hair-bundle motion. **(a)** Motions of the reticular lamina as a result of somatic motility of an apical OHC when stimulated with voltage steps. The measurement was taken from a 30-d-old gerbil hemicochlea with the TM detached from the OHC hair bundle. The cell was held at  $-70$  mV under whole-cell voltage-clamp. The patch electrode made contact with the basolateral membrane just above the nucleus of the cell. Movement was measured by the photodiode technique. Upward deflections in the trace represent depolarization. The response was filtered at 1,200 Hz. **(b)** Steady-state response from **a** was fitted with a second-order Boltzmann function (filled circles with solid line) and a slope function (solid line) was obtained as the derivative of the Boltzmann function. The bundle motion associated with somatic motility was also measured from the same cell, using the photodiode technique. Steady-state response was obtained and plotted in **b**. The response was also fitted with a second-order Boltzmann function (open circles with dashed line) and a slope function (dashed line) was obtained as the derivative of the Boltzmann function. **(c)** Bundle motion as a function of somatic motility. The magnitude of bundle motion is about one-half of that of somatic motility.

flow of calcium current through the mechanoelectrical transducer channel<sup>18</sup>. Another study shows that hair bundles of rat OHCs can produce a large force linked to adaptation of the mechanotransducer channels<sup>19</sup>. Such force can be fed back to the basilar membrane and could thereby amplify basilar membrane vibration<sup>6,7</sup>. Although the force generated by the hair bundle is almost 20- to 100-fold greater than that predicted by the gating-spring model for mammalian hair cells<sup>34</sup>, such force is approximately 5 to 10 times less than the force produced by OHC somatic motility (about 3–5 nN)<sup>25</sup>. The force production based on mechanotransducer channels is also accompanied by a change in stiffness of the bundle<sup>19</sup>. It is theoretically possible to construct a cochlear amplifier with an *in vivo* feedback pathway based on ciliary stiffness change<sup>35</sup>.

Our work demonstrates significant hair-bundle motions evoked by OHC electromotility. Yet, in the absence of electromotility (that is, in neonatal gerbil OHCs before the onset of somatic motility and in prestin-knockout mice), ciliary rotation linked to adaptation of the mechanotransducer channels was below the resolution limit of our system (~5 nm). The lack of bundle motion under the condition studied was not due to some malfunction of the mechanotransduction apparatus, since large mechanoelectrical transducer currents were observed. Although we can not rule out small mechanotransducer channel-based bundle motion below the resolution limit of our measurement system, the V-shaped or W-shaped staircase structure of the hair bundle with strong side-links connecting individual stereocilia is not well suited for ciliary rotation. The motility-associated bundle motion was large (over 800 nm), approximately ten times (20 dB) larger than the transducer channel-based ciliary rotation observed in non-mammalian hair cells<sup>8,9,13–15</sup>. The maximal sensitivity of the bundle motion was approximately 6.5 nm/mV, roughly one-half of that of OHC somatic motility. Voltage-evoked bundle motion of IHCs was reported in a recent study<sup>18</sup> using a two-chamber preparation. The IHC bundle motion observed was on the order of 13 nm. In our view, the possibility that such motion may have been mediated by OHC motility can not be completely ruled out. The motility-associated response we observed overshadows transducer channel-based mechanisms in OHCs.

It is not fully established how OHC length changes result in bundle motion. However, tilting of the cuticular plate during motility has been reported to occur at high frequencies in coil preparations<sup>36</sup>. Rotation of the reticular lamina as a result of OHC motility is also seen *in situ*<sup>32</sup>. Modeling work also supports the existence of reticular lamina rotation in response to OHC length change<sup>37</sup>. The bundle motion of unstimulated OHCs as a result of the somatic motility of adjacent OHCs provides direct evidence that tilting of the cuticular plate within the reticular lamina and rotation of the reticular lamina along its fulcrum at the pillar heads during OHC length change could produce bundle movement.

It has been proposed that OHC somatic motility<sup>3–5</sup> and stiffness change<sup>38</sup> are responsible for cochlear amplification in mammals. According to some theories, the force generated by OHC somatic motility amplifies the motion of the basilar membrane–organ of Corti complex<sup>39,40</sup>. These theories are supported by several observations, such as somatic motility upon ciliary deflection<sup>41</sup>, electromotility-driven movements of the reticular lamina and basilar membrane *in situ*<sup>32</sup>, and findings from experiments using prestin-knockout mice<sup>5,26</sup>. It has not yet been fully determined how active somatic movements of OHCs excite IHCs. Coupling OHC motility to basilar membrane and movements of the reticular lamina in an appropriate phase would certainly boost their displacements. In addition, the bundle motion associated with OHC somatic motility may provide a mechanism for OHC motility to boost the input to

IHCs. The V-shaped or W-shaped staircase structure of the OHC stereocilia is well suited for promoting mechanical coupling between the TM and reticular lamina, which can transfer motility-driven hair-bundle motion into the radial motion of the TM (data not shown). Such motion could amplify mechanical input to the IHC by increasing fluid motion in the gap between the TM and reticular lamina. This fluid flow stimulates the freestanding IHC cilia<sup>42</sup>. It is conceivable that fluid pumping by Hensen's stripe onto the closely apposed IHC cilia is the excitatory mechanism. It is therefore conceivable that the motility-associated hair-bundle motion may be part of cochlear amplification in mammals. Under this scheme, OHC somatic motility not only boosts basilar membrane vibration but also drives the hair-bundle motion, which can interact with the TM. Since the bundle motion is associated with somatic motility of OHCs, this scheme is consistent with studies using prestin-knockout mice<sup>5,26</sup>, which support motility-based amplification as the dominant mechanism in the mammalian cochlea.

The principal argument against somatic motility as the amplifier is that the low-pass filter characteristics of OHC membranes attenuate receptor potentials at high frequencies. Therefore, the receptor potentials would be too small to drive somatic motility<sup>6,7</sup>. It has been proposed, however, that extracellular potential changes within the organ of Corti could drive OHC motility at high frequencies<sup>43</sup>. These extracellular potentials are not filtered by the membrane. Measurements of basilar membrane vibration and extracellular potentials in the guinea pig cochlea at high frequencies provide evidence that those extracellular potentials can indeed drive OHC motors at high frequencies<sup>44–46</sup>. Extracellular OHC voltage responses at threshold are large and sharply tuned, and they are at least 100  $\mu$ V at threshold at 18 kHz<sup>45,46</sup>. Therefore, the potentials could be large enough to drive OHC motility. Furthermore, theoretical modeling also indicates that the piezoelectric property of OHCs can markedly increase the frequency response of OHCs<sup>47,48</sup>. Finally, characteristics of the mechanical load of OHCs within the organ of Corti may also improve the frequency response of OHCs<sup>49</sup>.

In summary, we have demonstrated that mammalian OHCs show large hair-bundle motion that is dependent on OHC somatic motility. Such bundle motion may boost the mechanical input to the IHC stereocilia through the radial motion of the TM. While forward-transduction-based hair-bundle motion may underlie cochlear amplification in non-mammals, mammals have evolved OHC somatic motility to boost basilar membrane vibration and to drive the bundle motion, thereby providing mechanical amplification of low-level signals in the mammalian inner ear.

## METHODS

Care and use of the animals in this study were approved by NIH grants and the Animal Care and Use Committee of Creighton University in Omaha, Nebraska.

**Preparation of the coil.** Gerbils ranging in age from 4 to 35 DAB and prestin-knockout mice ranging in age from 4 to 7 weeks after birth were used. The animals were decapitated following a lethal dose of sodium pentobarbital (200 mg/kg, intraperitoneal injection). After the cochlear wall was removed, the basilar membrane–organ of Corti complex was unwrapped from the modiolus, from the basal turn to the apical turn, as described elsewhere<sup>50</sup>. The coil was digested in L-15 medium (Invitrogen), containing 136 mM NaCl, 5.8 mM  $\text{NaH}_2\text{PO}_4$ , 5.4 mM KCl, 1.4 mM  $\text{CaCl}_2$ , 0.9 mM  $\text{MgCl}_2$ , 0.4 mM  $\text{MgSO}_4$  and 10 mM HEPES-NaOH (pH 7.4, 300 mmol/l), plus 0.06 mg/ml protease (type XXIV; Sigma). After the TM was lifted off to expose the hair bundles, the tissue was transferred to the experimental chamber. The coil was firmly attached to the bottom of the chamber by the weight of two thin platinum rods (0.5 mm in diameter), with one of their ends anchored in two small droplets of vacuum

grease on the bottom of the chamber. The tissue was mounted with the hair bundle facing upward toward the water-immersion objective. Details for preparing gerbil hemicochlea are given elsewhere<sup>31</sup>. The coil preparation (or hemicochlea) was bathed in L-15 medium in an experimental chamber mounted on the stage of an upright microscope (Leica DMLFSA) with Burleigh platform (Giblator). Quality control of coils and hemicochlea was based on the physical appearance of the preparation<sup>31</sup>. In either preparation, OHCs became swollen in less than 25 min after the organ of Corti was exposed to the extracellular medium. Therefore, all the data presented were collected within 20 min. Experiments were done at room temperature ( $22 \pm 2$  °C).

**Whole-cell voltage-clamp.** The coil preparation and the hemicochlea were both bathed in the L-15 medium. The pipette solution contained 140 mM CsCl (or KCl), 0.1 mM CaCl<sub>2</sub>, 3.5 mM MgCl<sub>2</sub>, 2.5 mM MgATP, 5 mM EGTA-KOH, 5 mM HEPES-KOH (pH 7.4 and 300 mmol/l). In some experiments, the ciliary area was perfused with artificial endolymph (150 mM KCl, 25 μM CaCl<sub>2</sub>, 1 mM sodium pyruvate, 5 mM D-glucose and 10 mM K<sub>2</sub>HPO<sub>4</sub> at pH 7.35 and 300 mmol/l) through a second pipette positioned approximately 20–30 μm away from the hair bundle, as described previously for turtle hair cell preparation<sup>13</sup>. The rate of perfusion and the distance of the perfusion pipette from the recording site were adjusted to ensure that the perfusion from this second pipette did not mechanically stimulate the bundle. The bath was perfused with fresh medium at a rate of 0.5 ml/min. Patch pipette resistance was 3–4 MΩ. Recordings were made in whole-cell voltage-clamp mode, using an Axopatch 200B patch-clamp amplifier (Axon Instruments). Series resistance was 8–14 MΩ, and about 75% of series resistance was compensated. The uncompensated voltage error was normally less than 4 mV at the largest voltage levels used since the membrane conductances were blocked. Currents were filtered at 2 kHz, and digitized at 10 kHz with a 16-bit A/D converter (Digidata 1322A) and pClamp 9.2 software (Axon Instruments). The cells were held at –70 mV. To measure mechanotransducer currents in the coil preparation, a fluid-jet technique was used to deflect the hair bundle. The home-made fluid jet was controlled by a Burleigh driver/amplifier (PZ-150M). Sinusoidal voltage commands (102 Hz) were used to drive the fluid jet. The fluid jet was positioned approximately 20–30 μm away from the stereocilia.

**Measurements of hair-bundle motion.** The preparation was obliquely illuminated by a 100-W lamp. The hair bundle was imaged using a 63× water-immersion objective (Leica) and magnified by an additional 20× relay lens. The magnified image of the tip of the bundle was then split into two paths: one path projected onto the photodiode (Hamamatsu) through a slit and another projected onto a CCD camera so that the bundle could be viewed at all times on a television monitor. During measurements, the magnified image of the tip of the bundle was positioned near the edge of the slit. The slit was rotatable, based on the orientation of the bundle. The output signal from the photodiode amplifier represented the motion of the tip of the hair bundle. The photodiode system had a 3-dB cutoff frequency of 1,200 Hz. The signal was then amplified by a 60-dB fixed-gain dc-coupled amplifier. The amplified signal was then low-pass filtered (400 or 1,200 Hz) before being delivered to one of the A/D inputs of a Digidata 1322A acquisition board (Axon Instruments) in a Microsoft Windows-based computer. The measurement system was capable of measuring bundle tip motions down to about 5 nm with 100 averages. Calibration of bundle motion was obtained by moving the slit a known amount (1 μm) using a piezo driver attached to the slit<sup>50</sup>.

To measure the motions of hair bundle and reticular lamina in the hemicochlea, we used a preparation in which the TM was detached from the OHC hair bundles. In this preparation, the hair bundle of OHCs is clearly visible on the cuticular plate and its motion is easy to measure under high magnification. We measured the hair-bundle motion and reticular lamina motion as described above, using the photodiode technique.

Note: Supplementary information is available on the Nature Neuroscience website.

#### ACKNOWLEDGMENTS

This work was supported by grants R01 DC 006496 and R21 DC 006039 to D.Z.Z.H. from the National Institutes on Deafness and Other Communicative Disorders (NIDCD). We would like to thank P. Dallos,

S. Neely, M.A. Cheatham and R. Hallworth for many helpful discussions and comments on an earlier draft of the manuscript. We thank J. Zuo for providing the prestin-knockout mice.

#### COMPETING INTERESTS STATEMENT

The authors declare that they have no competing financial interests.

Received 31 May; accepted 28 June 2005

Published online at <http://www.nature.com/natureneuroscience/>

- Dallos, P. The active cochlea. *J. Neurosci.* **12**, 4575–4585 (1992).
- Santos-Sacchi, J. New tunes from Corti's organ: the outer hair cell boogie rules. *Curr. Opin. Neurobiol.* **13**, 459–468 (2003).
- Brownell, W.E., Bader, C.R., Bertrand, D. & de Ribaupierre, Y. Evoked mechanical responses in isolated cochlear outer hair cells. *Science* **227**, 194–196 (1985).
- Kachar, B., Brownell, W.E., Altschuler, R. & Fex, J. Electromechanical shape changes of cochlear outer hair cells. *Nature* **322**, 365–368 (1986).
- Liberman, M.C. *et al.* Prestin is required for outer hair cell electromotility and the cochlear amplifier. *Nature* **419**, 300–314 (2002).
- Hudspeth, A.J. Mechanical amplification of stimuli by hair cells. *Curr. Opin. Neurobiol.* **7**, 480–486 (1997).
- Fettiplace, R., Ricci, A.J. & Hackney, C.M. Clues to the cochlear amplifier from the turtle ear. *Trends Neurosci.* **24**, 169–175 (2001).
- Crawford, A.C. & Fettiplace, R. The mechanical properties of ciliary bundles of turtle cochlear hair cells. *J. Physiol. (Lond.)* **364**, 359–379 (1985).
- Rüsch, A. & Thurm, U. Spontaneous and electrically induced movements of ampullary kinocilia and stereocilia. *Hear. Res.* **48**, 247–263 (1990).
- Martin, P. & Hudspeth, A.J. Active hair-bundle movements can amplify a hair cell's response to oscillatory mechanical stimuli. *Proc. Natl. Acad. Sci. USA* **96**, 14306–14311 (1999).
- Howard, J. & Hudspeth, A.J. (1987) Mechanical relaxation of the hair bundle mediates adaptation in mechano-electrical transduction by the bullfrog's saccular hair cell. *Proc. Natl. Acad. Sci. USA* **84**, 3064–3068 (1987).
- Benser, M.E., Marquis, R.E. & Hudspeth, A.J. Rapid, active hair bundle movements in hair cells from the bullfrog's sacculus. *J. Neurosci.* **16**, 5629–5643 (1996).
- Ricci, A.L., Crawford, A.C. & Fettiplace, R. Active hair bundle motion linked to fast transducer adaptation in auditory hair cells. *J. Neurosci.* **20**, 7131–7142 (2000).
- Assad, J.A., Hacohen, N. & Corey, D.P. Voltage dependence of adaptation and active bundle movement in bullfrog saccular hair cells. *Proc. Natl. Acad. Sci. USA* **86**, 2918–2922 (1989).
- Bozovic, D. & Hudspeth, A.J. Hair-bundle movements elicited by transepithelial electrical stimulation of hair cells in the sacculus of the bullfrog. *Proc. Natl. Acad. Sci. USA* **100**, 958–963 (2003).
- Gillespie, P.G. & Corey, D.P. Myosin and adaptation by hair cells. *Neuron* **19**, 955–958 (1997).
- Holt, J.R. *et al.* A chemical-genetic strategy implicates myosin-1c in adaptation by hair cells. *Cell* **108**, 371–381 (2002).
- Chan, D.K. & Hudspeth, A.J. Ca<sup>2+</sup>(+) current-driven nonlinear amplification by the mammalian cochlea *in vitro*. *Nat. Neurosci.* **8**, 149–155 (2005).
- Kennedy, H.J., Crawford, A.C. & Fettiplace, R. Force generation by mammalian hair bundles supports a role in cochlear amplification. *Nature* **433**, 880–883 (2005).
- Kros, C.J., Rüsch, A. & Richardson, G.P. Mechano-electrical transducer currents in hair cells of the cultured neonatal mouse cochlea. *Proc. Biol. Sci.* **249**, 185–193 (1992).
- Kennedy, H.J., Evans, M.G., Crawford, A.C. & Fettiplace, R. Fast adaptation of mechano-electrical transducer channels in mammalian cochlear hair cells. *Nat. Neurosci.* **6**, 832–836 (2003).
- He, D.Z.Z., Jia, S.P. & Dallos, P. Mechano-electrical transduction of outer hair cells studied in a gerbil hemicochlea. *Nature* **429**, 766–770 (2004).
- He, D.Z.Z., Evans, B.N. & Dallos, P. First appearance and development of electromotility in neonatal gerbil outer hair cells. *Hear. Res.* **78**, 77–90 (1994).
- Géléoc, G.S.G. & Holt, J.F. Developmental acquisition of sensory transduction in hair cells of the mouse inner ear. *Nat. Neurosci.* **6**, 1019–1020 (2003).
- Zheng, J. *et al.* Prestin is the motor protein of cochlear outer hair cells. *Nature* **405**, 149–155 (2000).
- Cheatham, M.A., Huynh, K.H., Gao, J., Zuo, J. & Dallos, P. Cochlear function in prestin knockout mice. *J. Physiol. (Lond.)* **560**, 821–830 (2004).
- Mammano, F., Kros, C.J. & Ashmore, J.F. Patch clamped responses from outer hair cells in the intact adult organ of Corti. *Pflügers Arch.* **430**, 745–750 (1995).
- Zhao, H.B. & Santos-Sacchi, J. Auditory collusio and a coupled couple of outer hair cells. *Nature* **399**, 359–362 (1999).
- Santos-Sacchi, J. Asymmetry in voltage-dependent movements of isolated outer hair cells from the organ of Corti. *J. Neurosci.* **9**, 2954–2962 (1989).
- Santos-Sacchi, J. On the frequency limit and phase of outer hair cell motility: effects of the membrane filter. *J. Neurosci.* **12**, 1906–1916 (1992).
- Richter, C.P., Evans, B.N., Edge, R. & Dallos, P. Basilar membrane vibration in the gerbil hemicochlea. *J. Neurophysiol.* **79**, 2255–2264 (1998).
- Mammano, F. & Ashmore, J.F. Reverse transduction measured in the isolated cochlea by laser Michelson interferometry. *Nature* **365**, 838–841 (1993).
- He, D.Z.Z. *et al.* Chick hair cells do not exhibit voltage-dependent somatic motility. *J. Physiol. (Lond.)* **546**, 511–520 (2003).

34. van Netten, S.M. & Kros, C.J. Gating energies and forces of the mammalian hair cell transducer channel and related hair bundle mechanics. *Proc. Biol. Sci.* **267**, 1915–1923 (2000).
35. McMullen, T.A. & Mountain, D.C. Model of dc potentials in the cochlea: effects of voltage-dependent cilia stiffness. *Hear. Res.* **17**, 127–141 (1985).
36. Reuter, G., Gitter, A.H., Thürm, U. & Zenner, H.P. High frequency radial movements of the reticular lamina induced by outer hair cell motility. *Hear. Res.* **60**, 236–246 (1992).
37. Dallos, P. Organ of Corti kinematics. *J. Assoc. Res. Otolaryngol.* **4**, 416–421 (2003).
38. He, D.Z.Z. & Dallos, P. Somatic stiffness of cochlear outer hair cells is voltage-dependent. *Proc. Natl. Acad. Sci. USA* **96**, 8223–8228 (1999).
39. Neely, S.T. & Kim, D.O. A model for active elements in cochlear biomechanics. *J. Acoust. Soc. Am.* **79**, 1472–1480 (1986).
40. de Boer, E. Mechanics of the cochlea: modeling efforts. in *The Cochlea* (eds. Dallos, P., Popper, A.N. & Fay, R.R.) 258–317 (Springer-Verlag, New York, 1996).
41. Evans, B.N. & Dallos, P. Stereocilia displacement induced somatic motility of cochlear outer hair cells. *Proc. Natl. Acad. Sci. USA* **90**, 8347–8351 (1993).
42. Dallos, P., Billone, M.C., Durrant, J.D., Wang, C. & Raynor, S. Cochlear inner and outer hair cells: functional differences. *Science* **177**, 356–358 (1972).
43. Dallos, P. & Evans, B.N. High-frequency motility of outer hair cells and the cochlear amplifier. *Science* **267**, 2006–2009 (1995).
44. Fridberger, A. *et al.* Organ of Corti potentials and the motion of the basilar membrane. *J. Neurosci.* **24**, 10057–10063 (2004).
45. Kössl, M. & Russell, I.J. The phase and magnitude of hair cell receptor potentials and frequency tuning in the guinea pig cochlea. *J. Neurosci.* **12**, 1575–1586 (1992).
46. Murugasu, E. & Russell, I.J. The effect of efferent stimulation on basilar membrane displacement in the basal turn of the guinea pig cochlea. *J. Neurosci.* **16**, 325–332 (1996).
47. Spector, A.A., Brownell, W.E. & Popel, A.S. Effect of outer hair cell piezoelectricity on high-frequency receptor potentials. *J. Acoust. Soc. Am.* **113**, 453–461 (2003).
48. Weitzel, E.K., Tasker, R. & Brownell, W.E. Outer hair cell piezoelectricity: frequency response enhancement and resonance behavior. *J. Acoust. Soc. Am.* **114**, 1462–1466 (2003).
49. He, D.Z.Z. Mechanical responses of cochlear outer hair cells. in *Biophysics of the Cochlea* (ed. Gummer, A.W.) 181–184 (World Scientific, Singapore, 2003).
50. He, D.Z.Z. Relationship between the development of outer hair cell electromotility and efferent innervation: a study in cultured organ of Corti of neonatal gerbils. *J. Neurosci.* **17**, 3634–3643 (1997).